Chapter 1
Insights into the Mechanism of Gas Sensor Operation

Aleksander Gurlo

Abstract Since the development of the first models of gas detection on metal-oxide-based sensors much effort has been made to describe the mechanism responsible for gas sensing. Despite progress in recent years, a number of key issues remain the subject of controversy; for example, the disagreement between the results of electrophysical and spectroscopic characterization, as well as the lack of proven mechanistic description of surface reactions involved in gas sensing. In the present chapter the basics as well as the main problems and unresolved issues associated with the chemical aspects of gas sensing mechanism in chemiresistors based on semiconducting metal oxides are addressed.

> *"Sensors have a 'life cycle' consisting of preparation, activation, operation with deactivation and, possible, regeneration. Thus understanding the performance in terms of reaction and conductance mechanisms is only a part of the total understanding of a sensor."*
>
> Dieter Kohl, *Sensors and Actuators* 1989, 18, 71.

A. Gurlo (✉)
Fachbereich Material- und Geowissenschaften, Technische Universitaet Darmstadt, Darmstadt, Germany
e-mail: gurlo@materials.tu-darmstadt.de

M. A. Carpenter et al. (eds.), *Metal Oxide Nanomaterials for Chemical Sensors*, Integrated Analytical Systems, DOI: 10.1007/978-1-4614-5395-6_1,

1.1 Chemiresistors: From Semiconductor Surfaces to Gas Detectors

Since the early 1920s numerous investigations have demonstrated the influence of the gas atmosphere on conductivity, free carrier mobility, surface potential, and work function on a number of semiconductors (see summary of early works in [1–13]). This led to the understanding that the surface of semiconductors is highly sensitive to chemical reactions and chemisorptive processes [3, 14–20] and resulted finally in the "theory of surface traps" (Brattain and Bardeen [21]), "boundary layer theory of chemisorption" [10, 22, 23] (Engell, Hauffe and Schottky) and "electron theory of chemisorption and catalysis on semiconductors" (Wolkenstein [5–7, 24]). They laid also the theoretical foundations for the subsequent development of metal-oxide-based gas sensors.

Although from this understanding to the use of semiconductors as gas sensors "was, in principle, a small step" [25], the idea of using the changes in conductivity of a semiconducting metal oxide for gas detection was not conceived until the middle of the 1950s. The earliest written evidence came in 1956, in the Diploma Thesis performed in Erlangen under supervision of Mollwo and Heiland and entitled "Oxygen detection in gases changes in the conductivity of a semiconductor (ZnO)" [26], the results discussed later in [1, 27]: "If one exposes a zinc oxide layer which has been given a previous heating at 500 K in a high vacuum to oxygen at a constant pressure, the conductivity falls very rapidly initially and more slowly later. If one then increases the oxygen pressure suddenly, the current of the conductivity exhibits a kink when plotted as a function of the time. In this change the slopes immediately before and immediately after the kink point are proportional to the partial pressure of oxygen. One can use this effect to relate a known and an unknown concentration of oxygen often even under conditions in which one has a mixture of gases…" (cited from Ref. [1]). In 1957, Heiland showed that the "well-conducting surface layer on zinc oxide crystals provides a new, very sensitive test for atomic hydrogen" [28] and Myasnikov demonstrated that ZnO films can be used as a highly-sensitive oxygen-analyzer [29]. Later he developed this "to the method of semicondutor probes", which allows for "studying free radical processes" and for detecting "free active particles and to measure their concentration under stationary and non-stationary conditions in gases and liquids" [30]. However, the conditions under which ZnO was able to operate as a "sensing device" were far from the real ambient conditions (and, accordingly, from a practical application); the "sensitive" effects were observed: (i) in vacuum conditions, exposed to oxygen or hydrogen, (ii) after "activation" or "sensitization" of the surface by heating in H_2 and in UHV.

The practical use of metal-oxide-based gas sensors in normal ambient conditions was not considered until 1962, when Seiyama et al. reported that a ZnO film can be used as a detector of inflammable gases in air [31] (see also [32]), and Taguchi claimed that a sintered SnO_2 block can also work in the same way [33] (for the history of TGS (Taguchi Gas Sensor) sensors, see [34]). The latter

approach became very successful, leading to the foundation of the first sensor company (Figaro Engineering Inc.), which established mass production and started selling the TGS sensors in 1968.

Since then, many different metal oxides have been investigated as sensing materials (see, for example, Ref. [35] for a comprehensive review), however, tin dioxide (SnO_2)—alone or "activated" with small quantities of noble metals/their oxides (Pd, Pt, Au)—has remained the most commonly used and the best-understood prototype material in commercial gas sensors [36] as well as in the basic studies of the gas sensing mechanism [35–43].

1.2 Characterization Methodology: From Prototype Surfaces to Operating Sensors

The detailed characterization of metal oxide sensors requires the "simultaneous measurement of the gas response and the determination of molecular adsorption properties for a better understanding of gas sensing mechanisms" [44]. This measurement can be done either on clean and well-defined surfaces in ultrahigh vacuum (UHV) conditions or at temperatures and pressures that mimic real sensor operating conditions ("in situ" [45]). Continuous progress has been made during the past few years for the latter strategy, i.e. toward the use of in situ and operando spectroscopic techniques.

The "crossing of interests" [46] and "bridges of physics and of chemistry across the semiconductor surface" [47] determined experimental methodology applied for the gas-semiconductor studies in general and gas sensing studies in particular in the course of the last 50 years.

The first systematic methodological approach ("design concept for chemical sensors") in gas sensing-studies was explicitly formulated in 1985, in a series of papers entitled "Development of chemical sensors: empirical art or systematic research?" ([48–50], see also [51]]).

The underlying concept was that by "studying the surface of single crystals under well-defined conditions, one might try to achieve a better separation of parameters influencing the properties of gas sensors" [52]. The reactions were addressed by surface spectroscopic methods under ultra-high-vacuum (UHV) conditions on well-defined "prototype" structures while the sensor performance was tested under realistic measuring conditions on the structures of practical importance ("sensors").

This "comparative approach" advanced the basic understanding of surface reactions and the corresponding conduction mechanism responsible for gas sensing. However, it showed also the limits of surface science in gas-sensing studies and led to the understanding that if spectroscopic and electrical data are not obtained simultaneously, they must be obtained (i) under the same conditions and (ii) on identical samples. A comprehensive description of surface reactions on SnO_2 published in 1989 resulted from simultaneous thermal desorption

spectroscopy (TDS; i.e. reactive scattering of a molecular beam) and conductance measurements [52]. These measurements were applied to SnO_2 single crystals and thin evaporated films exposed to a certain dose of CH_3COOH, CO or CH_4 in UHV conditions while at the sensor operating temperature.

As an alternative to sensing studies on single crystals or thin films, sensing characterization studies have focused on a combination of electrical measurements with spectroscopic investigations of catalysis reactions on *polycrystalline, high surface-area materials* with the aim to "link semiconductor studies with catalytic studies" [9]. However, most of the studies were performed under conditions far from the real working conditions of sensors (for the summary of numerous studies on semiconducting metal oxides, see references [4, 13, 53]). Besides spectroscopic and catalytic (kinetic) investigations (SnO_2: kinetic studies of CO oxidation [54], IR spectroscopic studies of water, CO_2 and CO adsorption [55], (summarized in Ref. [56]), EPR investigations of oxygen adsorption, [57], (reviewed in references [58, 59])), the improvements were concentrated on devising systems and in situ cells for combined (i.e., performed under the same conditions on "identical" samples) and simultaneous electrical, catalytic and spectral investigations.

These activities, however, were overlooked by the sensor community at that time, as in situ electrical characterization of realistic ("polycrystalline") samples, namely, the Hall effect measurements (1982 [60]), changes in work function (CPD) by the Kelvin method (1983 [61]), ac impedance spectroscopy (1991 [62, 63]), simultaneous work function change and conductance measurements (1991 [64]) were preferred for studying the mechanism of operating sensors [99].

Later, this approach was followed systematically in the number of works (reviewed in references [38, 65], recent works in references [66–70] and references therein) to elucidate a mechanism of gas detection on SnO_2-based sensors. Local electronic properties (e.g., the density of states in the region near the band gap) of a sensing material were determined by scanning tunnelling microscopy and spectroscopy (STM-STS) in vacuum conditions [71–73] or under N_2, CO and NO_2 (at room temperature) [74].

By the end of the 1990s, the spectroscopic techniques for gas-sensing studies were differentiated according to conditions under which they can be applied: those that may be applied "under in situ real operation conditions of the sensors" and those that may be applied "under ideal conditions far away from real practical world" [75]. This differentiation subsequently resulted in the systematic combination of phenomenological and spectroscopic measurement techniques under working conditions of sensors [38], and thus lead to the in situ and operando methodology.

Continuous progress has been made during the past few years for the latter strategy, that is, the use of in situ and operando spectroscopic techniques (see [76, 77]):

- In situ spectroscopy: *spectroscopic characterization of sensing materials under operation conditions or conditions relevant to operation conditions; herein, the sensing performance of this material may be not characterized or may be characterized in a separate experiment,*

- Operando spectroscopy: *spectroscopic characterization of an active sensing element in real time and under operating conditions with the simultaneous read-out of the sensor activity and simultaneous monitoring of gas composition.*

These definitions determine the boundary conditions under which an "operando" experiment is performed:

1. on a *sensing element,* which itself is a complex device and consists of several parts: in solid-state devices with an electrical response, for example, the sensing layer is deposited onto a substrate to which electrodes for an electrical read-out are attached ("transducer"); therefore the assessment of their interfaces is of paramount importance for understanding the overall sensing mechanism;
2. *in real time:* a sensor is devised to respond to the changes in the gas atmosphere as fast as possible; accordingly, it demands a fast spectroscopic response;
3. *under operating conditions:* these can vary from ambient conditions (RT and atmospheric pressure) to high temperatures and pressures;
4. *with simultaneous read-out of sensor activity:* the gas concentration to be measured is transduced by the sensor into an electrical or other convenient output, depending on the modus operandi of sensor (optical, mechanical, thermal, magnetic, electronic, or electrochemical) and the transducer technology;
5. *with simultaneous monitoring of gas composition*; on-line gas analysis in gas sensing plays a twofold role: (i) the output compositions and concentrations provide data about reaction products and possible reaction paths and (ii) the input concentration verifies the sensor input data (concentration of the component to be detected).

The operando methodology couples electrical ("phenomenological") and spectroscopic techniques and, aims to correlate the sensor activity with the spectroscopic data obtained under the same conditions on the same sample (Fig. 1.1). In an ideal case, one would obtain four types of information: (i) gas-phase changes (and reaction products) from on-line gas analysis, (ii) species adsorbed on the surface, (iii) changes in the oxide surface and lattice, and (iv) sensor activity.

1.3 Mechanism of Gas Detection: Never Ending Story About Oxygen

Epigraph

> Due to the electron affinity of oxygen, the electron can be transferred to the chemisorbed oxygen and, consequently, there will be no chemisorbed oxygen atoms, but ions, in the surface
>
> K. Hauffe, *Adv. Catal.* **1955***, 7,* 213– 257.

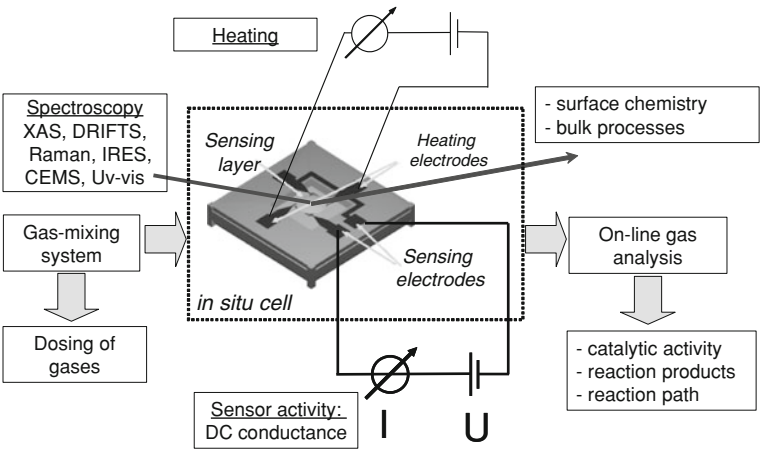

Fig. 1.1 Methodological approach for simultaneous spectroscopic and electrical ("phenomenological") characterisation of metal-oxide-based gas sensors. Modified from ref. [76]

Since the development of the first models of gas detection on metal-oxide-based sensors [78, 79] much effort has been made to describe the mechanism responsible for gas sensing (see, for example, [80–82]). Despite progress in recent years, a number of key issues remain the subject of controversy; for example, the disagreement between electrophysical and spectroscopic investigations, as well as the lack of a proven mechanistic description of surface reactions involved in gas sensing.

Nowadays, the influence of the gas atmosphere on the electrical transport properties of semiconductors and, accordingly, the operation of metal-oxide-based gas sensors is currently described by the combination of two different models; they are the ionosorption and the reduction-reoxidation mechanisms (Table 1.1). The *ionosorption model* considers only the space-charge effects/changes of the electric surface potential that results from the "ionosorption" of gaseous molecules. The *reduction-reoxidation model* explains the sensing effects by changes in the oxygen stoichiometry, that is, by the variation of the amount of the (sub-) surface oxygen vacancies and their ionization. The latter involves explicitly the diffusion of oxygen (or oxygen vacancies) from/in the bulk of the sensing material.

1.4 Oxygen Ionosorption

The electrical conductivity and work function can be described as collective physical properties of semiconductors which are changed by an ionosorption process and are accessible to measurement. *The key in the mechanistic description of gas sensing is "oxygen ionosorption" and reaction of reducing gases with ionosorbed oxygen ions*.

Table 1.1 Gas sensing mechanism on SnO_2 according to ionosorption and oxygen vacancy models

Gas detection	Ionosorption model	Oxygen vacancy model
Oxygen	$O_2(ads) + e^-(CB) \leftrightarrow O_2^-(ads)$ $O_2^-(ads) + e^-(CB) \leftrightarrow O_2^{2-}(ads) \leftrightarrow 2O^-(ads)$	$2V_O^{\bullet} + O_2\ (gas) + 2e^-(CB) \leftrightarrow 2O_O^{\times}$
CO/presence of oxygen	$CO\ (gas) + O^-(ads) \leftrightarrow CO_2(gas) + e^-(CB)$	$CO\ (gas) + O_O^{\times} \leftrightarrow CO_2(gas) + V_O^{\times}$ $V_O^{\times} \leftrightarrow V_O^{\bullet} + e^-(CB)$
CO/absence of oxygen	$CO\ (gas) \leftrightarrow CO^+(ads) + e^-(CB)$	$V_O^{\bullet} \leftrightarrow V_O^{\bullet\bullet} + e^-(CB)$
NO_2	$NO_2\ (gas) + e^-(CB) \leftrightarrow NO_2^-(ads)$	$NO_2(gas) + V_O^{\bullet} \leftrightarrow NO_2^-(ads) + V_O^{\bullet\bullet}$ $2NO_2(gas) + O_2^-(ads) + V_O^{\bullet} \leftrightarrow 2NO_3^-(ads) + V_O^{\bullet\bullet}$
Water vapour	$H_2O\ (gas) + O^-(ads) + 2Sn_{Sn}^{\times} \leftrightarrow 2(Sn_{Sn}^{\times} - OH) + e^-(CB)$ $H_2O\ (gas) + Sn_{Sn}^{\times} + O_O^{\times} \leftrightarrow (Sn_{Sn}^{\times} - OH) + OH_O^{\bullet} + e^-(CB)$	$H_2O\ (gas) + 2Sn_{Sn}^{\times} + O_O^{\times} \leftrightarrow 2(Sn_{Sn}^{\times} - OH) + V_O^{\bullet} + e^-(CB)$

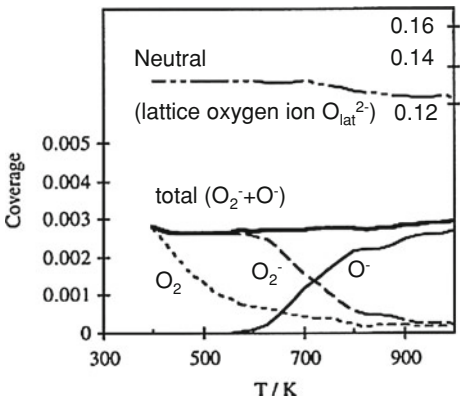

Fig. 1.2 The simulated equilibrium coverages of the oxygen species. The transition from O_2^- to O^- is calculated to be around 700 K (intersection at 427 °C). Copyright Elsevier, reproduced with permission from Ref. [100]

The oxygen influence on the electrical conductivity and work function is very well documented. For SnO_2, for example, exposure of single crystals (Ref. [83] and refs therein), polycrystalline samples (porous films [84], powders [57], pressed bars[85]) as well as one dimensional nanostructures [86, 87] to oxygen leads to the (i) decrease in the electrical conductivity and in the concentration of conduction electron density (Hall effect measurements [57]), (ii) increase in the work function observed in UHV conditions (XPS/UPS [88]) and under atmospheric pressure (simultaneous Contact Potential Difference, CPD, and conductance measurements [84]). Similar effects have been also observed on TiO_2 and ZnO (see early publications on TiO_2 [89, 90] [91] and on ZnO [3, 92–95]).

The magnitude of the changes depends strongly on the oxide temperature (see for example [85] and [84]), particle size and pre-treatment (history). On high-surface area and reduced samples the changes are much higher in comparison to single crystals and oxidised samples. The reduced samples show activity at temperatures as low as room temperature (r.t.), for oxidised samples higher temperatures (>100 °C) are needed. This difference between oxidised and reduced samples is usually ignored by the "ionosorption theory".

Because the detailed mechanism of oxygen adsorption cannot be derived directly from electrophysical investigations[96], the chemistry of adsorbed surface oxygen on SnO_2 was adapted from the "ionosorption model" [97–100]. It was assumed that the thermally stimulated processes of oxygen adsorption, dissociation and charge transfer involve only conduction electrons [4, 81]:

$O_2(\text{gas}) \leftrightarrow O_2(\text{ads})$	*Physisorption*
$O_2(\text{ads}) + e^-(\text{CB}) \leftrightarrow O_2^-(\text{ads})$	*Ionosorption*
$O_2^-(\text{ads}) + e^-(\text{CB}) \leftrightarrow O_2^{2-}(\text{ads}) \leftrightarrow 2O^-(\text{ads})$	*Ionosorption*
$O^-(\text{ads}) + e^-(\text{CB}) \leftrightarrow O^{2-}(\text{ads})$	*Ionosorption*
$O^{2-}(\text{ads}) \leftrightarrow O^{2-}(\text{1st bulk layer})$	*Diffusion*

The nature of the ionised oxygen species is assumed to depend on the adsorption temperature (Fig. 1.2). At low temperatures (150–200 °C) oxygen adsorbs on SnO_2 non-dissociatively in its molecular form (as charged O_{2ads}^- ions). At high temperatures (between 200 and 400 °C or even higher) it dissociates to atomic oxygen (as charged O_{ads}^- or O_{ads}^{2-} ions) [4, 37, 75, 80, 81, 98, 99, 101]. Neutral oxygen species such as physisorbed oxygen, $O_{2,\,phys}$, are assumed not to play any role in gas sensing. The same holds for the lattice oxygen ions, O_{lat}^{2-}, in bulk materials at temperatures not high enough for fast oxygen exchange reactions (see detailed discussion below).

At this point, a problem of semantics starts to bring additional confusion, especially in the operational use of the terms "charged" species and the "charge transfer" at the surface. In semiconductor physics, the charge transfer implies by definition the transfer of free charge carriers, that is, conduction electrons or holes. Accordingly, the species that influence the electrical conductivity are regarded as "charged" or "ionized". They are represented by free oxygen ions. The species that do not influence the conductivity are regarded as "neutral". They are represented by physisorbed oxygen molecules.

The phenomenological model describes the oxygen ionosorption on an n-type semiconductor as follows:

- ionosorbed oxygen species are formed due to the transfer of conduction electrons from the semiconductor;
- they can be regarded as free oxygen ions which are electrostatically stabilized in the vicinity of the surface;
- there are no other adsorbed oxygen species besides physisorbed oxygen and oxygen ions;
- physisorbed oxygen is electrically neutral and oxygen ions are electrically active ("charged") species.

The simplified picture showing the influence of adsorption on surface conductivity and work function is as follows. An oxygen molecule becomes physisorbed at the surface. In the next step, an electron from the oxide's conduction band is trapped at the adsorbed oxygen molecule. The adsorbed oxygen molecule and surface itself become negatively charged. The flow of electrons from the semiconductor into the chemisorbed layer, without any diffusion of ionic species at the same time, induces a space charge between the interior of the semiconductor and its surface. The negative surface charge is compensated by a positive charge and a space-charge layer forms below it. This positive space-charge layer has reduced electron densities as compared to the bulk and is called an "electron-depleted layer or a charge depleted layer". As a result the energy band, pertaining to the surface, bends upwards with respect to the Fermi level. This causes the creation of barriers on the surface, ($q\Delta V_S > 0$), due to the increasing work function, ($q\Delta V_S > 0$), and decreasing surface conductance ($G = G\exp(-q\Delta V_S/kT)$ (Fig. 1.3). The process of charge transfer continues until equilibrium is reached and a steady state is achieved. To prevent very high double-layer potentials, the total amount of the "charged" species is limited to 10^{-5}–10^{-3} monolayer which corresponds approximately to 1 V of the surface potential V_S (this is the so-called

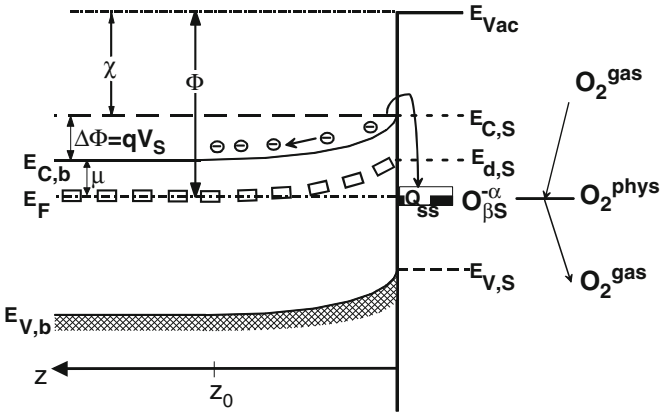

Fig. 1.3 Band bending on an n-type semiconductor after ionosorption of oxygen. Work functions Φ of semiconductors contain three contributions; e.g. the energy difference between the Fermi level and conduction band in the bulk $(E_C - E_F)_b$, band bending qV_S (q denotes elementary charge) and electron affinity χ: $\Phi = (E_C - E_F)_b + qV_S + \chi$ (due to the definition, $V_S = E_{C,S} - E_{C,B}$). For ionosorption the work function follows only the change in band bending ($\Delta\Phi = q\Delta V_S$). The z_0 denotes the depth of the depletion region; μ—the electrochemical potential; $E_{V,B}$ and $E_{V,S}$—valence band edge in the bulk and at *the surface, respectively;* $E_{d,S}$—*donor level at the surface;* $E_{C,B}$ *and* $E_{C,S}$—*conductance band* edge in the bulk and at the surface, respectively; E_F—Fermi level; $O_{2,gas}$ is an oxygen molecule in the ambient atmosphere; $O_{2,phys}$—a physisorbed oxygen species; $O^{-\alpha}_{\beta S}$—a chemisorbed oxygen species ($\alpha = 1$ and $\alpha = 2$ for singly and doubly ionised forms, respectively; $\beta = 1$ and $\beta = 2$ for atomic and molecular forms, respectively)

Weisz limitation, see original [18] and discussion in [4]). Within the framework of this concept, the operation of SnO_2-based sensors is described as follows: oxygen adsorbs in a delocalized manner, trapping electrons from the conduction band and forming ions—"charged" molecular ($O_2^{-\ ads)}$ and atomic (O^-ads, O_2^-ads) species—electrostatically stabilized at the surface in the vicinity of metal cations. This happens under real working conditions of sensors, between 100 and 450 °C, at atmospheric pressure, at 20.5 vol. % background oxygen.

Reducing gases, like CO, react with the oxygen ions (by either Eley–Rideal or Langmuir–Hinshelwood mechanism) freeing electrons that return to the conduction band.

The ionosorption theory explains also the increase in the sensing performance with decreasing crystal size. Firstly, the reactivity of nanomaterials is mainly determined by the so-called "smoothly scalable" size-dependent properties which are related to the fraction of atoms at the surface [102]. As the crystal size decreases, the surface-to-volume ratio increases proportionally with the inverse of the crystal size. The increase in the total surface-to-volume ratio with respect to the size decrease generates more "reactivity" due to a dominant surface-like behavior caused by an increased fraction of atoms at the surface [102]. Thus, all properties which depend on the surface-to-volume ratio change continuously and

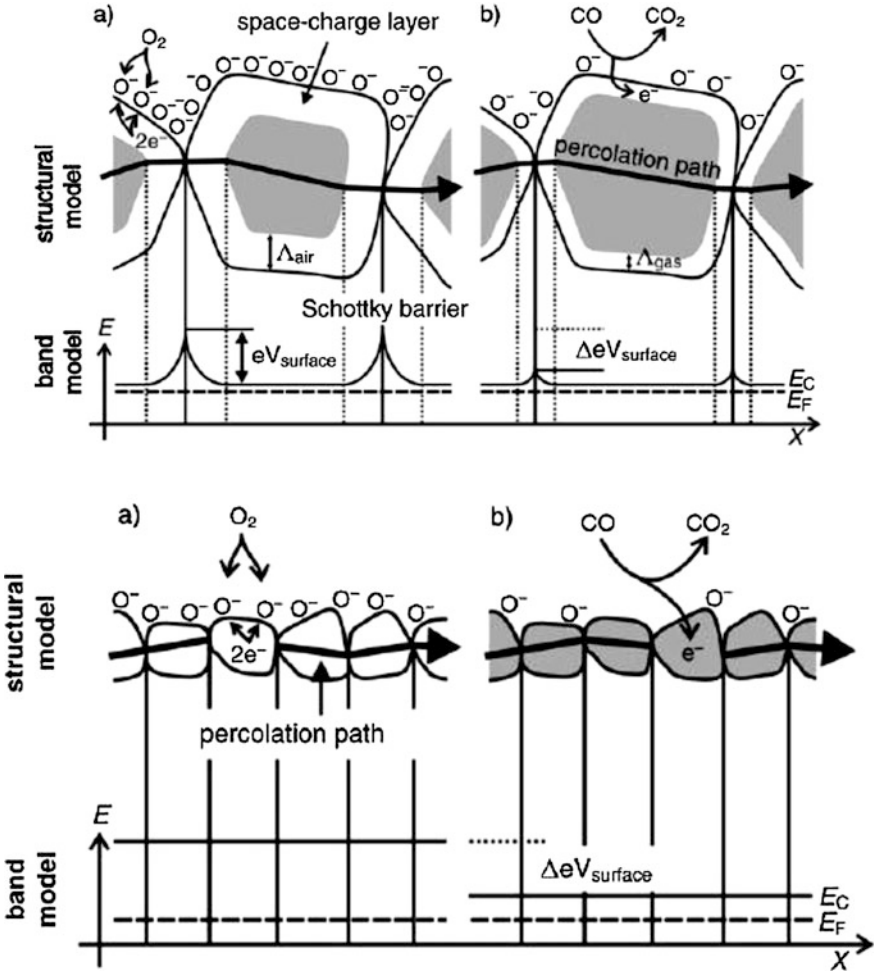

Fig. 1.4 The mechanism controlling the conductivity change and its magnitude depends on the ratio between grain size (D) and Debye screening length (Λ). If $D > 2\Lambda$, the depletion of the surface between the grain boundaries controls the conductivity. In this case low response to the analyte is expected as only a small part of the semiconductor is affected by interaction with analyte. If $D \leq 2\Lambda$, the whole grain depleted and changes in the surface oxygen concentration affects the whole semiconductor resulting in high response. Copyright Wiley–VCH, reproduced with permission from Ref. [43]

extrapolate rapidly at very low crystal sizes. As a consequence, nanoparticles with increased surface-to-volume ratio are expected to be more reactive and accordingly, more gas sensitive.

With decreasing crystal size there is also a transition from a partly to a completely charge depleted particle that can be observed, depending on the ratio between the crystal and the Debye screening length L_D (Λ in Fig. 1.4) (for calculation, see for

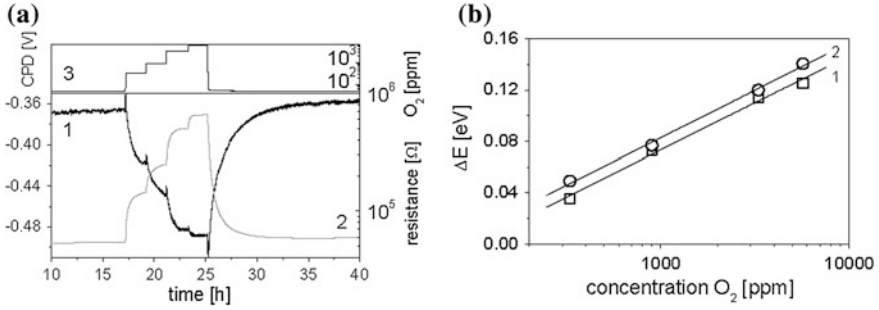

Fig. 1.5 **a** The contact potential difference (CPD $= -\Delta\Phi$) *1* and the resistance *2* have been recorded at different O_2 concentrations *3* on the nanocrystalline SnO_2 at 400 °C in dry nitrogen at atmospheric pressure (adapted from Ref. [84]). **b** Calculated from **a** work function change ($\Delta\Phi$) *1* and band bending ($q\Delta V_S = kTln(G_0/G)$) *2* changes. Copyright Wiley–VCH, reproduced with permission [145]

example [37, 103]). For partly depleted particles, when surface reactions do not influence the conduction in the entire layer, the conduction process takes place in the bulk region. Formally, two resistances occur in parallel, one influenced by surface reactions and the other not; the conduction is parallel to the surface, and this explains the limited sensitivity [37, 39]. Fully depleted particles possess higher sensitivity as the charge depletion layer fully impacts the conduction channel within the nanoparticle, thus achieving better performance in gas exposure experiments [43].

Summarizing, the atomic charged oxygen ion (O^-ads) is assumed to be of particular importance in gas sensing because "the O^- ion appears to be more reactive of the two possibilities and thus more sensitive to the presence of organic vapours or reducing agents…" [81]. *Accordingly, "there are two important questions to resolve here: First, under what conditions does O^- dominate over O_2^-? Second, what is the total surface charge as a function of … temperature and partial oxygen pressure?"* [81] *As a consequence, ambitious efforts have been made* (i) *to calculate the surface coverage by different types of ionosorbed oxygen* [6, 104–106] (Fig. 1.2*) and* (ii) *to correlate the overall conductance of the sensors with the chemical state of charged oxygen species at the surface* [37, 107].

The contradiction arises when connecting the main statements of the ionosorption model to common chemical sense and spectroscopic findings.

A first example of this is to note that oxygen ionosorption should be reflected in *equal* changes in the work function and band bending, $kTln(G_0/G) = q\Delta V_S = \Delta\Phi$ (see also Fig. 1.3). These values can be independently obtained, for example, in the simultaneous CPD (here $\Delta V_{CPD} = -\Delta\Phi = q\Delta V_S$) and conductance measurements (here $q\Delta V_S = kTln(G_0/G)$, see an example in [38].

However, even if one can measure *formal* evidence for the pure oxygen ionosorption ($kTln(G_0/G) = \Delta\Phi$, Fig. 1.5, the transient changes observed ($q\Delta V_s = 0$, $\Delta\Phi = 0$ after 50 h) reflects very slow surface processes. These slow changes are in sharp contrast to the fast charging expected at the oxide surface (see Ref. [108], charging takes less than 5 ms even at 250 K) and this discrepancy is not explained by "ionosorption theory".

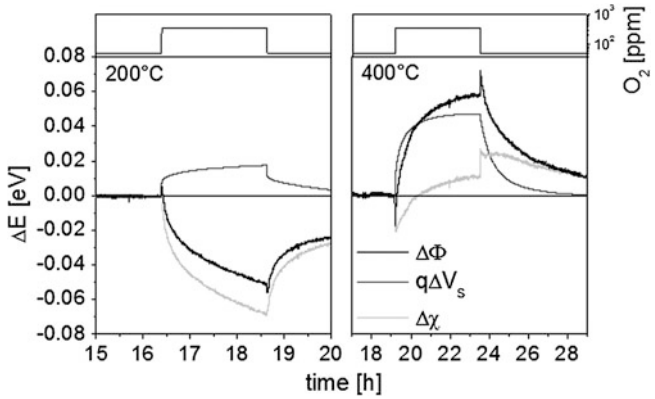

Fig. 1.6 Changes in work function (*black*), band bending (*dark grey*) and electron affinity (*light grey*) due to 300 ppm O_2 (-—-) at 200 °C (*left*) and at 400 °C (*right*). Copyright Elsevier, reproduced with permission from Ref. [67]

The results shown in Fig. 1.5 strongly suggest that at 400 °C all other species, besides ionic ones, can be regarded as being of secondary importance. However, at 200 °C a completely different behavior of the changes of the work function appear. This is illustrated by Fig. 1.6 where changes in work function, band bending and electronic affinity due to a pulse of 300 ppm oxygen are displayed for 200–400 °C, respectively. The most important difference is the strong decrease in electronic affinity at 200 °C. Such effects did not appear at 400 °C. As shown in Ref. [38], the changes in electronic affinity are connected with the formation or loss of dipolar species between adsorbate and adsorbent accompanied by localized bonding. Therefore, in order to get an explanation of the experimental results we have to allow for the possibility of dipole formation arising from the adsorption of neutral molecular oxygen species (Fig. 1.7). These species are neglected in all mechanistic description of gas sensing on semiconducting metal oxides.

A critical look at the available experimental data shows that the concept of oxygen ionosorption is based exclusively on phenomenological measurements. Despite trying for a long time, there has not been any convincing spectroscopic evidence for "ionosorption". Neither superoxide ion O_2^-, nor charged atomic oxygen O^-, nor peroxide ions O_2^{2-}, nor CO^+ have been observed under real working conditions of sensors (see a recent review [109]).

With regard to the two main forms of charged oxygen species on the surface (superoxide ion O_2^- and charged atomic oxygen O^-) and widely used in the mechanistic description of gas sensing properties and modelling of oxide conduction mechanism, it appears that:

1. The superoxide ion (O_2^-) has been observed only after low-temperature adsorption <150 °C on reduced SnO_2;
2. There has not been any spectroscopic evidence for the formation of charged atomic oxygen (O^-) on SnO_2.

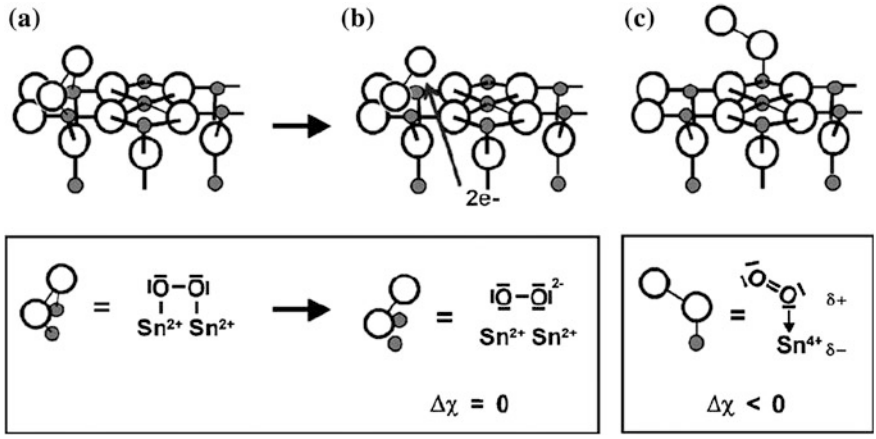

Fig. 1.7 Adsorption of O_2 on a reduced SnO_2 (110) surface. There is a stable state for a twisted conformation on a fourfold Sn^{2+} site (**a**) It is expected to accept negative charge under building of ionosorbed species and thus without influence on electron affinity (**b**) A stable conformation tilted from the normal, where a Lewis acid/base interaction leads to a local dipole with a negative partial charge on the tin and thus to a decrease in χ, is also reported (**c**) Copyright Elsevier, reproduced with permission from Ref. [67]

Moreover, several findings, such as (i) the formation of superoxide ion (O_2^-)only at low adsorption temperatures(<150 °C) on reduced SnO_2, (ii) absence of a high-temperature oxygen desorption (peak at 400–550 °C, attributed to adsorbed oxygen) if the superoxide-ion is present at the surface, (iii) decrease in oxygen intensity with increasing evacuation temperature; herewith the amount of O_2 desorbed is equal to the number of superoxide ion centres, (iv) correlation between TPD, EPR, IR and electrophysical studies on reduced SnO_2, allows us to conclude that the *superoxide ion does not undergo transformations into charged atomic oxygen at the surface and represents a dead-end form of low-temperature oxygen adsorption on reduced metal oxide.*

As known, the superoxide ion can undergo the following chemical changes on the surface: (i) lose an electron (to the CB) and leave as gaseous O_2 and (ii) gain an additional electron (becoming a peroxide ion O_2^{2-}), followed by cleaving to form atomic oxygen and the lattice oxygen anion (O^{2-}). According to the spectroscopic data (there is no evidence either for peroxide ion or for charged atomic oxygen) the transformation from superoxide ion to atomic oxygen does not happen on SnO_2. This indicates two competing channels for oxygen adsorption—molecular and dissociative. A similar mechanism has been recently postulated for TiO_2 [110] and Ag [111]. On TiO_2, only η^2-coordinated dioxygen decomposes to oxygen adatom and a filled oxygen vacancy (in contrast, the η^1-coordinated dioxygen desorbs at 410 K [110]). On Ag, upon heating, physisorbed oxygen transforms into molecular chemisorbed I α-O_2 ("end-form") which does not dissociate into the atomic form due to the high conversion barrier; only molecular chemisorbed II β-O_2 ("transformable form") accessible only through a direct interaction from the gas phase (and not accessible from physisorbed form) dissociates into atomic oxygen [111].

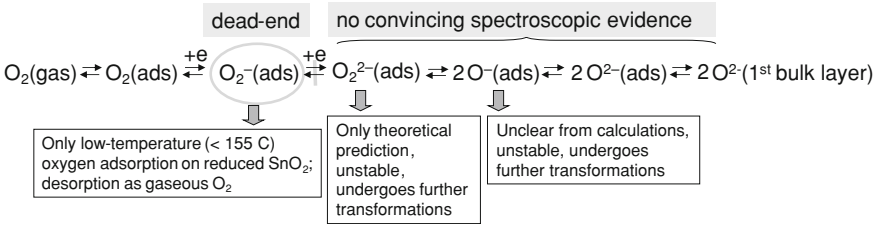

Fig. 1.8 Scheme of oxygen interaction with metal oxides showing the superoxide ion as a dead-end form. Modified from Ref. [145]

The long sought efforts to quench "high-temperature" oxygen species (claimed to represent charged atomic oxygen—O^-) has not yielded any measureable success. No such paramagnetic species have been observed on high-temperature oxygen treated oxides (TiO_2, SnO_2, ZnO) [95, 112, 113]. Moreover, the EPR evidence of the surface O^- species formed due to oxygen adsorption is very contradictory. Furthermore, from a review of the literature there isn't convincing evidence of their formation on n-type semiconducting oxides due to their direct interaction with dioxygen. Likewise, it is not possible to connect the high-temperature peak in the TPD spectra and the change in the conductivity with the formation of surface O^- species. Consequently, the conclusions on O^- formation on SnO_2 are not supported by any spectroscopic data. Accordingly, the picture of oxygen adsorption on SnO_2 has to be modified in the following way (Fig. 1.8).

1.5 Oxygen-Vacancy Model (Reduction-Reoxidation Mechanism)

This model focuses on oxygen vacancies at the surface, which are considered to be "the determining factor in the chemiresistive behavior" [114]. Tin dioxide, the most extensively investigated sensing material, is oxygen-deficient and, therefore, an n-type semiconductor, whose oxygen vacancies act as electron donors. Alternate reduction and reoxidation of the surface by gaseous oxygen (Mars—van Krevelen mechanism)control the surface conductivity and therefore the overall sensing behaviour. In this model, the mechanism of CO detection is represented as follows: (i) CO removes oxygen from the surface of the lattice to give CO_2, thereby producing an oxygen vacancy; (ii) the vacancy becomes ionized, thereby introducing electrons into the conduction band and increasing the conductivity; (iii) if oxygen is present, it fills the vacancy; in this process one or more electrons are taken from the conduction band, which results in a decrease in conductivity.

Numerous experimental and theoretical works have evaluated the reduction-reoxidation mechanism (see, for example, references [52, 114–119]); this mechanism still dominates in almost all spectroscopic studies (see, for example, references [120–125], Table 1.2). For example, it was found that oxygen promotes

Table 1.2 Some examples of main finding from in situ and operando case studies of gas sensing on semiconducting metal oxides

Method	Oxides	Gases	Main findings
IRES	WO_3, $AlVO_4$ and Co_3O_4 [124]	O_2 in N_2, C_3H_6 and acetone in air	Ionisation of oxygen vacancies
DRIFTS	CdGeON [147, 148]	O_2 in N_2	Filling of oxygen vacancies; change of the Ge coordination number
XAS	SnO_2 and Pd/SnO_2 [136, 149]	CO and H_2 in N_2	Sn^{4+} and Pd^{2+} reduction as secondary processes, CO and H_2 oxidation by ionosorbed oxygen
XAS	Pt/SnO_2 [150, 151]	CO in N_2, H_2S	Variation in Pt oxidation state in reducing and oxidising atmospheres
XAS	SnO_2; Pt/SnO_2 [152, 153]	Air, CO/air, CO/N_2, O_2	Variation in Pt oxidation state in reducing and oxidising atmospheres
CEMS	Bi_2O_3-SnO_2 [152, 153]	He, CO/He, CH_4/He	Oxidation by lattice oxygen atoms, formation of oxygen vacancies
FTIR	TiO_2, SnO_2, In_2O_3, WO_3 [154–159]	CO_2, CO, O_2, O_3, NOx	Variations of the free carriers density
FTIR	SnO_2 [123, 128]	O_2/N_2, CO/air, He/air	Photoionisation of ionised oxygen vacancy with increasing oxygen content
	SnO_2, MoOx-SnO_2, Pd/SnO_2, WOx-SnO_2 [129, 160–163]	O_2, CO, NO, NO_2	Formation of oxygen vacancies and their ionisation
DR UV-vis	SnO_2 [164]	O_2, hydrazine	Formation of oxygen vacancies and their ionisation
CEMS	SnO_2 and Ru, Pt, Pt/SnO_2 [165, 166]	NO/argon, air	Formation of oxygen vacancies and their ionisation
	SnO_2 and Pd/SnO_2 [121]	CO/N_2, air	Formation of Sn (II) as indicator of oxygen vacancy formation
EPR	SnO_2; Ru, Pt, Pt/SnO_2 [120, 165–168]	Dry and humid air, CO in air and N_2, NO/Ar, H_2	Formation of oxygen vacancies and their ionisation

water vapour dissociation on SnO_2 at 330–400 °C [126]: an increase in the concentration of hydroxyl groups (peaks at 3640 cm^{-1}) was observed for low oxygen (2000 ppm) and water vapour (3 ppm) concentrations and evolved towards saturation. This effect was explained by the reaction:

$$H_2O\,(\text{gas}) + O^-(\text{ads}) + 2Sn_{Sn}{}^{\times} \leftrightarrow 2(Sn_{Sn}{}^{\times} - OH) + e^-(CB)$$

At first sight this seems to provide evidence for the ionosorption model. However, this effect (i.e. the increase in the concentration of hydroxyl groups during oxygen exposure) can be explained just as well, by completely different processes within the framework of the oxygen vacancy model. For example, an EPR signal of single ionised oxygen vacancies ($V_O^{\bullet}$) at 1.89 was observed after wet

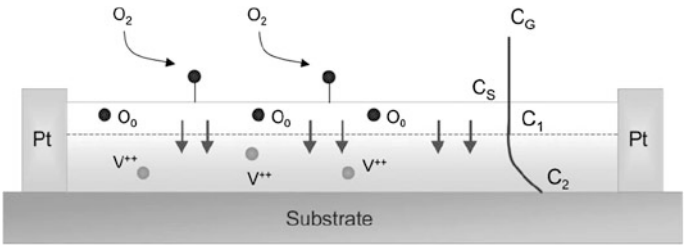

Fig. 1.9 One-dimensional model of oxygen diffusion in nanowires. According to the ionosorption model, adsorbed oxygen creates a depletion region close to the surface (dashed line) and then a fast change of R_{NW} is observed. The new equilibrium between oxygen in the environment, C_G, and the concentration of oxygen at both the nanowire surface, C_S, and its external shell, C_1, creates a gradient with the inside C_2 favoring ion migration into the bulk. This diffusion is associated with long-term drifts of R_{NW}. Copyright Wiley–VCH, reproduced with permission from Ref. [134]

air treatment of SnO_2 at 200 °C [127]. Accordingly, the observed influence of water and oxygen can be described by the two reactions:

$$38;\, H_2O\ (\text{gas}) + 2Sn_{Sn}{}^{\times} + O_O{}^{\times} \leftrightarrow 2(Sn_{Sn}{}^{\times} - OH) + V_O{}^{\bullet} + e^-(CB)$$

$$38;\, 2V_O{}^{\bullet} + O_2\ (\text{gas}) + 2e^-(CB) \leftrightarrow 2O_O{}^{\times}$$

However, the problems associated with oxygen adsorption and detection of reducing gases in an oxygen-free atmosphere are questioning the validity of the reduction-reoxidation model (see detailed discussion below).

As we mentioned above, ionosorbed oxygen has never been observed in operando and in situ studies on metal oxide sensors under working conditions [123, 124]. By contrast, operando and in situ spectroscopy provides very strong evidence of the reaction and ionization of oxygen vacancies under operating conditions of sensors [120–124].

The in situ FT-IR studies [123, 128] of SnO_2 under working conditions (at 375–450 °C) showed an increase of the intensity in the broad band in the region of 2300–800 cm^{-1} (so-called X-band) with increasing oxygen content. The proximity of the absorption edge with respect to the ionization energy of the second level of oxygen vacancies (1400–1500 cm^{-1} ~ 170–180 meV) is indicative of the electronic transition from this level to the conduction band (i.e. photoionisation of $V_O^{\bullet}$ to $V_O^{\bullet\bullet}$)[129]. Accordingly, this band can serve as an indicator of the electron concentration in the neighborhood of oxygen vacancies in the SnO_2. Similar effects were observed on Ga_2O_3, $AlVO_4$, WO_3 [124]. However, this interpretation was considered to be in contrast to the early electrophysical measurements on SnO_2 [130] which showed that the donor levels in SnO_2 are located at around 30–150 meV below the conduction band, and will be completely ionized at the sensor operating temperatures [131, 132]. The next problem is related to (i) the ionization of oxygen vacancies and consequently, and (ii) to the diffusion processes in the oxide lattice. For SnO_2, for example, it is assumed that the surface defects do not

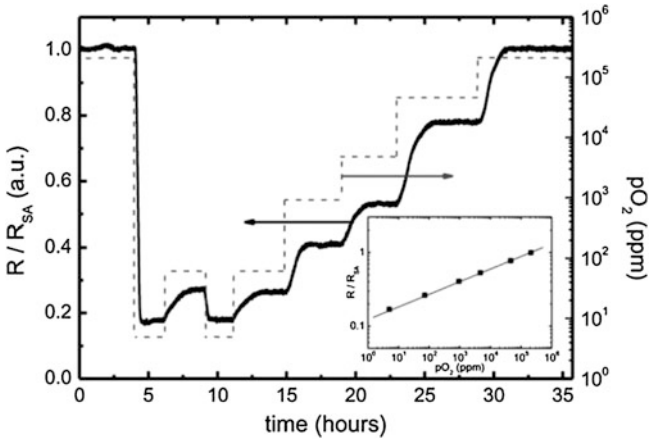

Fig. 1.10 Response of one SnO_2 nanowire with r = 20 nm to increasing oxygen partial pressure at room temperature (T = 298 K). Resistance is normalized to the experimental value in synthetic air environment. (Inset) log−log plot of resistance as function of oxygen partial pressure. A linear behavior of slope n = 1/6 is observed. Copyright Wiley–VCH, reproduced with permission from Ref. [134]

act as electron donors; they have to migrate a small distance into the bulk to become ionized [52]. The diffusion coefficients for this process are low, and, accordingly, the defects are immobilized at the operating temperatures [116]. Nevertheless, diffusion at grain boundaries and at the surface can be much faster than bulk diffusion [12].

A different situation seems to appear in quasi-one-dimensional SnO_2 structures (nanowires) [133, 134], where the oxygen adsorption involves two steps (i) healing of oxygen vacancies by adsorbed oxygen (fast) and (ii) diffusion of as-formed oxygen ions in the bulk healing (annealing) oxygen vacancies (slow) (Fig. 1.9).

Surprisingly, even at room temperature an exponent of 1/6 was found in the power law for the oxygen partial pressure dependence of the sensor signal (i.e. conductivity) indicating an intrinsic case in the defect chemistry of SnO_2 (Fig. 1.10) [116]:

$$38;\frac{1}{2}O_2 + V_O^{\bullet\bullet} + 2e^{/} \leftrightarrow O_O$$

$$38;\left[e^{/}\right] = 2^{1/3}K_O{}^{-1/3}p_O{}^{-1/6}, \text{ considering the electroneutrality condition}$$

$$38;\left[e^{/}\right] = 2[V_O^{\bullet\bullet}]$$

These findings contrast with bulk film studies which have shown that (i) the surface exchange reaction, i.e. the incorporation of adsorbed oxygen together with the fast electron transfer, is the rate-determining step [118] and (ii) significant oxygen exchange is observed on SnO_2 only at temperatures above 400 C [135].

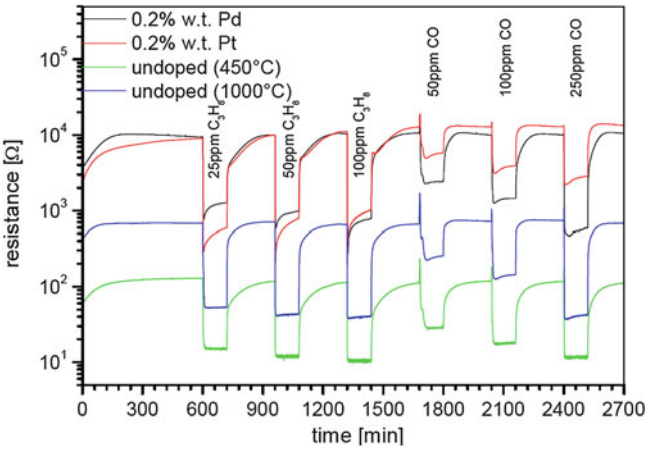

Fig. 1.11 Transient resistance change of undoped, Pd and Pt doped SnO_2 sensors in oxygen free atmosphere (N_2 balance) [146]. Note, that the sensor resistance recovers its initial value after removing the target gas from the surrounding atmosphere

1.6 Reduction as a Secondary Process: an Open Issue of Detection of Reduction Gases in Oxygen-Free Conditions

The mechanism of detection of reducing gases in oxygen-free atmospheres requires consideration of the following four experimentally confirmed observations:

1. Recovery of sensor resistance to its initial value in an inert gas (N_2, Ar, He) after removing a reducing gas (CO, CH_4, H_2) from the test atmosphere.
2. Missing correlation between the degree of oxide reduction and the magnitude of gas sensing response.
3. Missing correlation between the gas combustion (oxidation) and the magnitude of gas sensing response.
4. Decrease of sensor signals (relative resistance change) with increasing oxygen concentration.

We have to note that a lack of experiments does not allow addressing properly these issues; some important points are discussed below.

Let us take as an example of CO detection in the oxygen-free conditions (alternating CO/N_2 and N_2 flows): What happens when CO is removed from the surrounding atmosphere? From electrical measurements one knows that the sensor resistance (or conductance) recovers its initial value (Fig. 1.11). However, within the framework of the reduction-reoxidation mechanism, gaseous oxygen is required for the reverse process ("vacancy refilling"). Unfortunately, the consideration of this problem has been avoided in spectroscopic studies by alternating

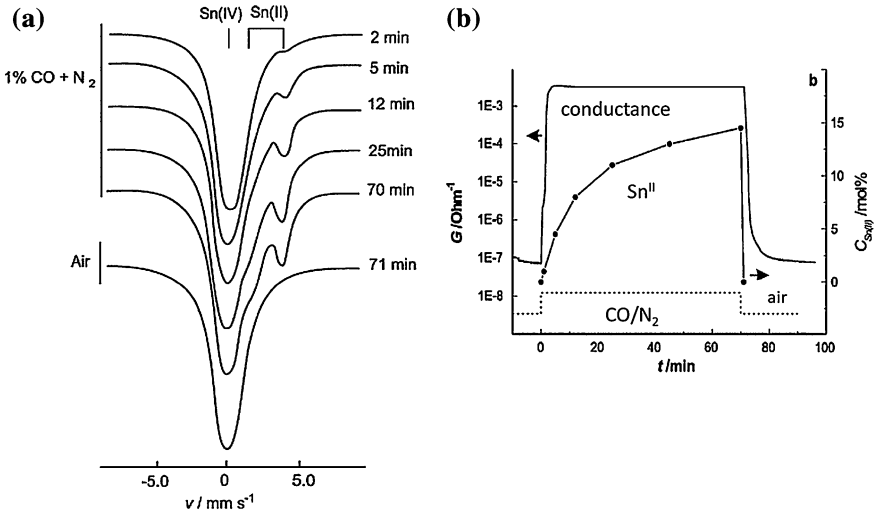

Fig. 1.12 **a** Mössbauer spectra of SnO_2 in a 1 % CO/N_2 atmosphere and then in dry air at 380 °C; **b** Electrical response of SnO_2 and change of Sn(II) concentration in 1 % CO/N_2 and dry air at 380 °C under 4 l/h gas flow rate. Copyright the Royal Chemical Society, reproduced with permission from Ref. [121]

CO/N_2 (or Ar) and O_2/N_2 (or Ar) flows, whereas "realistic" conditions require alternating CO/N_2 (or Ar) and N_2 (or Ar) flows.

The oxide reduction as well as reduction/reoxidation of catalytic additives like Pd and Pt seems to be a secondary process that is not connected with the overall sensor response. Figure 1.12 a and b shows the electrical response combined with a change of Sn(II) concentration revealed by in situ Mössbauer spectra for nanocrystalline SnO_2 in the presence of CO and dry air at 380 °C. It was shown that the conductance changes simultaneously with the change of the tin oxidation state (which in turn indicates the formation of oxygen vacancies). A rapid and pronounced increase in Sn(II) spectral contribution was observed just after CO admission into the reactor. The Sn(II) component disappeared 1 min after air admission. It was also noted that (i) a very low Sn(II) content (1 mol %) was sufficient for the conductance to change by 1000 times and (ii) a further increase of Sn(II) concentration up to 14 mol % under exposure to CO did not significantly change the conductance. Similar findings have been also reported for H_2 detection with Pd-promoted SnO_2 sensors. Figure 1.13 [136] show the correlation between the electrical conductance and the oxidation states of Pd and Sn during the cycling of Pd–SnO_2 film in H_2 and O_2 gas mixtures. At 373 K, the conductance changes without any variation of the Pd and Sn oxidation states. At higher temperatures, the oxidation state of Pd varies considerably depending on the atmospheric composition. However, there is no direct correlation between the conductance and the oxidation states of Pd and Sn, i.e. even at 573 K the conductance changes by several orders of magnitude without any measurable variation of the oxidation

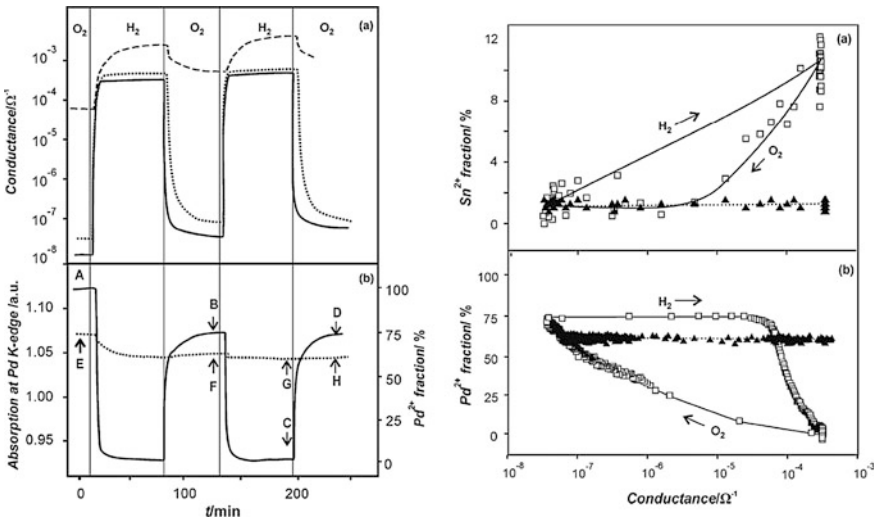

Fig. 1.13 (On the *left*) Variation of the electrical conductance **a** normalized absorption at Pd K-edge (b, *left scale*) and Pd^{2+} fraction in the Pd^{2+}/Pd^{0} mixture (b, *right scale*) for Pd–SnO_2 film at 573 K (*solid lines*) and 373 K (*dotted lines*) during the alternative exposure to 20 % O_2 in He and 1000 ppm H_2 in He. The broken line corresponds to pure SnO_2 at 573 K. (On the right) Operando XAS and conductance studies. The correlation between the conductance of Pd–SnO_2 film and the oxidation states of tin **a** and palladium **b** at 573 K (*white squares*, *solid lines*) and 373 K (*black triangles*, *dotted lines*). Fraction of Pd^{2+} is the concentration of Pd^{2+} in the Pd^{2+}/Pd^{0} mixtures; the fraction of Sn^{2+} is the concentration of Sn^{2+} in the Sn^{2+}/Sn^{4+}mixture. The arrows indicate the direction in which the system changes during exposure to H_2 and O_2 Copyright the Royal Chemical Society, reproduced with permission from Ref. [136]

states of both metals. These results indicate that oxidation and reduction of Pd nanoparticles and SnO_2 matrix are the secondary processes, which are not responsible for the sensitivity to H_2.

No direct correlation exists between sensor activity (i.e. sensor signal) and consumption of target gases obtained from the on-line gas analysis. As demonstrated in Fig. 1.14 herein at 200 °C the sensor shows relatively high activity in C_3H_8 detection (sensor signal is about 6–400 ppm C_3H_8) the combustion, however, is almost negligible [137]. The same also holds for higher temperatures and other analytes. Several recent works have also demonstrated that there has been no direct correlation between sensor (SnO_2, TiO_2…) response to CO and the CO_2 production ("catalytic activity") [138–140].

The strong argument is coming from the observation that in the "oxygen-free" atmosphere the sensor response (i.e. relative change in the conductance) is even higher than in "oxygen" containing atmosphere (Fig. 1.15). To explain these findings, an assumption about the formation of ionosorbed donor-like CO^{+} species is made (see, for example [141] and Fig. 1.16). However, like in the case of ionosorbed oxygen species we face here a problem of common chemical understanding and missing spectroscopic evidence.

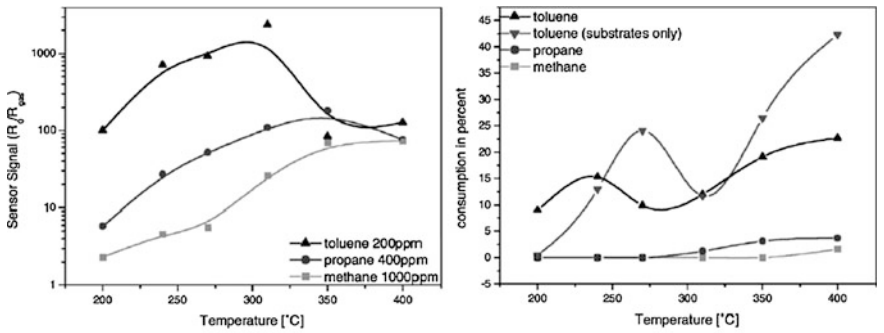

Fig. 1.14 (*Left*) Sensor signal of SnO_2 sensors exposed to different analytes in dry air dependent on operating temperature of sensors and (*right*) overall gas combustion measured by on-line PAS Copyright Elsevier, reproduced with permission from Ref. [137]

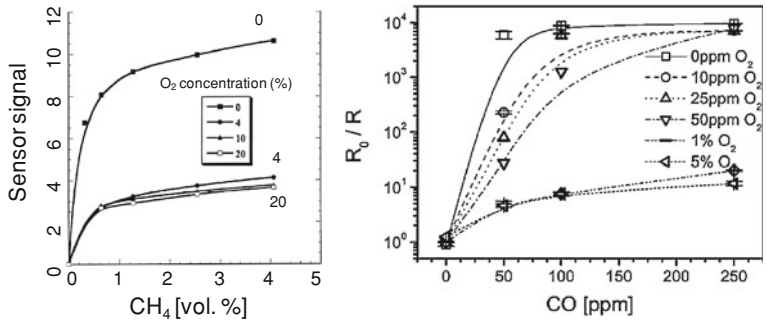

Fig. 1.15 (*left*) Relative change in the conductance (sensor signal, defined as $(G_{CH4}\text{-}G_0)/G_0$, where G_{CH4} and G_0 are the conductance values measured at 450 C under CH_4 supporting gas, respectively.) for undoped SnO_2 as a function of CH_4 concentrations for different O_2 concentrations (N_2 balance). Copyright Elsevier, reproduced with permission from Ref. [85]. (*Right*) Sensor signal of a 0.2 wt % Pt doped SnO2 thick film sensor at 300 C as a function of CO concentration for different O_2 concentrations (0, 10, 25, 50 ppm, 1 and 5 %). Copyright Elsevier, reproduced with permission from Ref. [141]

1.7 Summary and Outlook

Since the development of the first models of gas detection on metal-oxide-based sensors much effort has been made to describe the mechanism responsible for gas sensing. Despite progress in recent years, a number of key issues remain the subject of controversy; for example, the disagreement between electrophysical and spectroscopic investigations, as well as the lack of proven mechanistic description of surface reactions involved in gas sensing. The state-of-the-art description and understanding of gas sensing on metal oxides cannot explain all effects observed on *operating* metal oxide sensors.

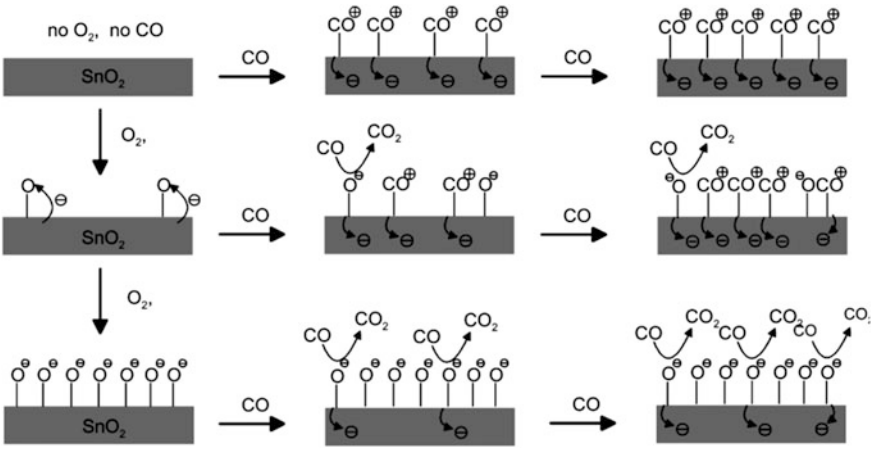

Fig. 1.16 Schematic representation CO interaction with SnO_2 as function of the O_2 concentration: in the absence of O_2, CO adsorbs as electron donor and leads to a decrease of the sensor resistance. In the presence of O_2, CO reacts mainly with adsorbed O_2 species. The contribution of each mechanism depends on the O_2 concentration. Copyright Elsevier, reproduced with permission from Ref. [141]

Obviously, our ability for understanding fundamental physicochemical phenomena is limited by dominant physicochemical paradigms. Accordingly, the interpretation of spectroscopic data depends on the model a priori chosen for the mechanistic description.

Besides general applicability for describing the mechanism of gas sensing on semiconducting metal oxides, the ionosorpion model works very well in explaining also quite unobvious results under a priori made unproven assumptions; typical examples are:

- higher response to reducing gases such as CO in absence of oxygen compared with that in the presence of oxygen; here the assumption is made about the formation of ionosorbed donor-like CO^+ species (see, for example [141]);
- large response for smaller crystals; obviously this interpretation does not involve and does not require the explicit formation of any ions at the surface. In case of the interaction with gaseous oxygen, the key is only the decrease of electron density (depletion) in the surface regions of a metal oxide; this effect is more pronounced in materials with higher surface/volume ratio (see, for example, Ref. [103]);
- reversible p- to n- and to p-type transition on semiconducting metal oxides induced by gas adsorption [142, 143].

The ionosorption theory fails to explain several important issues, among them:

1. the missing spectroscopic evidence as well as theoretical confirmation of ionosorbed oxygen species and
2. electron affinity changes due to the oxygen adsorption.

Excluding the electron transfer to adsorbed species by assuming the localization of electrons in solid material in close vicinity to adsorbed/gaseous species eliminates immediately the issue of missing spectroscopic evidence of oxygen ions. The polarizability effects can also be involved for explaining the competition between e.g. CO and oxygen: in the presence of CO, adsorbed O_2 molecules will also attract the electrons from the highly polarizable CO molecules thus reducing the O_2 strength to attract the conduction electrons [144]. This assumption can also explain large response for smaller crystals (see above). However, it fails to explain the higher response—meaning the increase in the conductance—to reducing gases such as CO in absence of oxygen compared with that in the presence of oxygen.

Even if numerous experimental and theoretical works have evaluated the reduction-reoxidation mechanism and this mechanism still dominates in almost all spectroscopic studies, the reduction-reoxidation model fails to explain

1. the missing correlation between the conductance of sensing materials and the degree of reduction *under operating conditions* (from operando studies);
2. kinetics of oxygen exchange;
3. recovery of the sensor resistance to its initial value after exposure to reducing gases in oxygen-free conditions where—according to the reduction-reoxidation mechanism, gaseous oxygen is required for the reverse process ("vacancy refilling");
4. lack of gaseous products of the oxidation of reducing gases (e.g. CO_2) from simultaneous on-line gas analysis.

References

1. Heiland G, Mollwo E, Stockmann F (1959) Electronic processes in zinc oxide. Solid State Phys 8:191–323
2. Many A, Goldstein Y, Grover NB (1971) Semiconductor surfaces. North-Holland Publishing Company, Amsterdam, 496
3. Morrison SR (1955) Surface-barrier effects in adsorption, illustrated by zinc oxide. Adv Catal 7:259–301
4. Morrison SR (1977) The chemical physics of surfaces, Plenum Press, New York, 415
5. Wolkenstein T (1960) Electron theory of catalysis on semiconductors. Adv Catal 12:189–264
6. Wolkenstein T (1987) Electronic processes on the surface of semiconductors during chemisorption, Consult Bur New York, 431
7. Wolkenstein T (1964) Elektronentheorie der Katalyse an Halbleitern, Verlin: VEB
8. Hauffe K (1955) Application of the theory of semiconductors to problems of heterogeneous catalysis. Adv Catal 7:213–57
9. Hauffe K (1955) Application of the semiconductor theory to problems of heterogeneous catalysis. Angewandte Chemie 67:189–207
10. Engell HJ, Hauffe K (1953) The boundary-film theory of chemisorption. Interpreting the reaction on the solid-gas interface (Die Randschichttheorie der Chemisorption . Ein Beitrag zur Deutung von Vorgängen an der Grenzfläche Festkörper/Gas). Zeitschrift fuer Elektrochemie und Angewandte Physikalische Chemie 57:762–73

11. Hauffe K (1955) Reaktionen in und an Festen Stoffen (Erste Auflage). Springer, Berlin, 696
12. Hauffe K (1966) Reaktionen in und an Festen Stoffen (Zweite Auflage). Springer, Berlin, 696
13. Kiselev VF, Krylov OV (1987) Electronic phenomena in adsorption and catalysis on semiconductors and dielectrics. Springer series in surface sciences, Springer, Berlin, 279
14. Roginskii SZ (1949) Principles of catalyst theory. Problemy Kinetiki i Kataliza 6:9–53
15. Wagner C (1950) The mechanism of the decomposition of nitrous oxide on zinc oxide as catalyst. J Chem Phys 18:69–71
16. Bevan DJ, Anderson MJS (1950) electronic conductivityconductivity and surface equilibria of zinc oxide. Discussions of the Faraday society 8:238–246
17. Boudart M (1952) Electronic chemical potential in chemisorption and catalysis. J Am Chem Soc 74:1531–5
18. Weisz PB (1953) Effects of electronic-charge transfer between adsorbate and solid on chemisorption and catalysis. J Chem Phys 21:1531–8
19. Morrison SR (1953) Changes of surface conductivity of germanium with ambient. J Phys Chem 57:860–3
20. Garrett CGB (1960) Quantitative considerations concerning catalysis at a semiconductor surface. J Chem Phys 33(4):966–979
21. Brattain WH, Bardeen J (1953) Surface properties of germanium. Bell Sys Tech J 32:1–41
22. Engell HJ (1954) Randschichteffekte an der Grenzfläche Hableiter/Vakuum und Halbleiter/Gasraum. Halbleiterprobleme 1:249–272
23. Hauffe K (1956) Gas reactions on semiconducting surfaces and space charge boundary layers. In: Kingston RH (ed) Semiconductor surface physics, University of Pennsylvania Press, Philadelphia 259–282
24. Vol'kenshtein FF (1949) Electronic theory of promotion and poisoning of ionic catalysts. Problemy Kinetiki i Kataliza 6(Geterogennyi Kataliz):66–82
25. Morrison SR (1982) Semiconductor gas sensors. Sens Actuators 2(4):329–341
26. Kefeli A (1956) Sauerstoffnachweis in Gasen durch Leitfähigkeitsänderung eines Halbleiters(zno). Diploma Thesis, Institut für Angewandte Physik, Universität Erlangen, Erlangen
27. Heiland G (1982) Homogeneous semiconducting gas sensors. Sens Actuators 2(4):343–61
28. Heiland G (1957) Effect of hydrogen on the electrical conductivity on the surface of zinc oxide crystals (Zum Einfluss von Wasserstoff auf die elektrische Leitfähigkeit an der Oberfläche von Zinkoxydkristallen). Zeitschrift fuer Physik 148:15–27
29. Myasnikov IA (1957) The relation between the electric conductance and the adsorptive and sensitizing properties of zinc oxide. I. Electron phenomena in zinc oxide during adsorption of oxygen. Zhurnal Fizicheskoi Khimii 31:1721–30
30. Kupriyanov LY (1996) Semiconductor sensors in physico-chemical studies. In: Middelhoek S (ed) Handbook of sensors and actuators, vol 4. Elsevier, Amsterdam p 412
31. Seiyama T, Kato A, Fujiishi K, Nagatani M (1962) A new detector for gaseous components using semiconductive thin films. Anal Chem 34:1502–1503
32. Seiyama T, Kagawa S (1966) Detector for gaseous components with semiconductive thin films. Anal Chem 38(8):1069–73
33. Taguchi N (1962) Gas-detecting device. Jpn Pat 45–38200
34. Chiba A (1992) Development of the TGS gas sensor. In: Yamauchi S (ed) Chemical sensor technology, Elsevier, Amsterdam pp 1–18
35. Eranna G, Joshi BC, Runthala DP, Gupta RP (2004) Oxide materials for development of integrated gas sensors—a comprehensive review. Crit Rev Solid State Mater Sci 29(3–4):111–188
36. Ihokura K, Watson J (1994) Stannic oxide gas sensors, principles and applications. CRC Press, Boca Raton p 187
37. Barsan N, Weimar U (2001) Conduction model of metal oxide gas sensors. J Electroceram 7(3):143–167
38. Barsan N, Weimar U (2003) Understanding the fundamental principles of metal oxide based gas sensorsgas sensors; the example of CO sensing with SnO_2 sensors in the presence of humidity. J Phys-Condens Matter 15(20):813–839

39. Gurlo A, Barsan N, Weimar U (2006) Gas sensors based on semiconducting metal oxidesmetal oxides. In: Fierro JLG (ed) Metal oxides: chemistry and applications, CRS Press, Boca Raton, pp 683–738
40. Ahlers S, Müller G, Doll T (2005) A rate equation approach to the gas sensitivity of thin film metal oxide materials. Sens Actuators, B: Chem 107(2):587–599
41. Park CO, Akbar SA (2003) Ceramics for chemical sensing. J Mater Sci 38(23):4611–4637
42. Korotcenkov G (2005) Gas response control through structural and chemical modification of metal oxide films: state of the art and approaches. Sens Actuators, B: Chem 107(1):209–232
43. Franke ME, Koplin TJ, Simon U (2006) Metal and metal oxide nanoparticles in chemiresistors: does the nanoscale matter? Small 2(1):36–50
44. Batzill M, Diebold U (2006) Characterizing solid state gas responses using surface charging in photoemission: water adsorption on SnO2(101). J Phys-Condens Matter 18(8):129–134
45. Bell NA, Brooks JS, Forder SD, Robinson JK, Thorpe SC (2002) Backscatter Fe-57 Mossbauer studies of iron(II) phthalocyanine. Polyhedron 21(1):115–118
46. Wolkenstein T (1969) Introduction. In: Hauffe K and Wolkenstein T (eds) Symposium on electronic phenomena in chemisorption and catalysis on semiconductors, Walter de Gruyter & Co, Berlin, pp 67–82
47. Weisz PB (1956) Bridges of physics and chemistry across the semiconductor surface. In: Kingston RH (ed) Semiconductor surface physics, University of Pennsylvania Press, Philadelphia, pp 247–258
48. Goepel W (1985) Entwicklung chemischer Sensoren: empirische Kunst oder systematischeForschung? Teil 2 (Development of chemical sensors: empirical art or systematic research? Part 2). Technisches Messen 52(3):92–105
49. Goepel W (1985) Entwicklung chemischer sensoren: empirische Kunst oder systematischeForschung? Teil 3 (Development of chemical sensors: empirical art or systematic research? Part 3). Technisches Messen 52(2):175–182
50. Goepel W (1985) Entwicklung chemischer sensoren: empirische Kunst oder systematischeForschung? (Development of chemical sensors: empirical art or systematic research?). Technisches Messen 52(5):175–82
51. Goepel W (1985) Chemisorption and charge transfer at ionic semiconductor surfaces: implications in designing gas sensors. Prog Surf Sci 20(1):9–103
52. Kohl D (1989) Surface processes in the detection of reducing gases with tin dioxide-based devices. Sens Actuators 18(1):71–113
53. Kiselev VF, Krylov OV (1985) Adsorption processes on semiconductor and dielectric surfaces I. Springer series in chemical physics, 287
54. Fuller MJ, Warwick ME (1973) Catalytic oxidation of carbon monoxide on tin(IV) oxide. J Catal 29(3):441–50
55. Thornton EW, Harrison PG (1975) Tin oxide surfaces. I Surface hydroxyl groups and the chemisorption of carbon dioxide and carbon monoxidecarbon monoxide on tin(IV) oxide. J Chem Soc, Faraday Trans 1: Phys Chem Condens Phases 71(3):461–72
56. Harrison PG (1989) Tin(IV) Oxide: surface chemistry, catalysis and gas sensing. In: Harrison PG (ed) Chemistry of Tin, Blackie, Glasgow
57. Mizokawa Y, Nakamura S (1975) ESR and electric conductance studies of the fine powdered tin dioxide. Jpn J Appl Phys 14(6):779–88
58. Che M, Tench AJ (1982) Characterization and reactivity of mononuclear oxygen species on oxide surfaces. Adv Catal 31:77–133
59. Che M, Tench AJ (1983) Characterization and reactivity of molecular oxygen species on oxide surfaces. Adv Catal 32:1–148
60. Ogawa H, Nishikawa M, Abe A (1982) Hall measurement studies and an electrical conduction model of tin oxide ultrafine particle films. J Appl Phys 53(6):4448–4455
61. Mizsei J, Harsanyi J (1983) Resistivity and work function measurements on Pd-doped SnO_2 sensor surface. Sens Actuators 4:397–402

62. Schierbaum KD, Weimar U, Goepel W, Kowalkowski R (1991) Conductance, work function and catalytic activity of SnO_2-based gas sensors. Sens Actuators, B: Chem B3(3):205–214
63. Gutierrez J, Ares L, Horillo MC, Sayago I, Agapito J, Lopez L (1991) Use of complex impedance spectroscopy in chemical sensor characterization. Sens Actuators B: Chem 4(3–4):359–363
64. Mizsei J, Lantto V (1991) Simultaneous response of work function and resistivity of some SnO_2-based samples to H_2 and H_2S. Sens Actuators B: Chem 4(1–2):163–168
65. Kappler J (2001) Characterization of high-performance SnO_2 gas sensorsgas sensors for CO detection by in-situin-situ techniques (Ph.D. Thesis, University of Tübingen) Aachen: Shaker Verlag
66. Oprea A, Moretton E, Barsan N, Becker WJ, Wollenstein J, Weimar U (2006) Conduction model of SnO_2 thin films based on conductance and Hall effect measurements. J Appl Phys 100(3):033716
67. Sahm T, Gurlo A, Barsan N, Weimar U (2006) Basics of oxygen and SnO_2 interaction; work function change and conductivity measurements. Sens Actuators, B: Chem 118(1–2):78–83
68. Sahm T, Gurlo A, Barsan N, Weimar U, Madler L (2005) Fundamental studies on SnO_2 by means of simultaneous work function change and conduction measurements. Thin Solid Films 490(1):43–47
69. Gurlo A, Barsan N, Oprea A, Sahm M, Sahm T, Weimar U (2004) An n- to p-type conductivity transition induced by oxygen adsorption on alpha-Fe_2O_3. Appl Phys Let 85(12):2280–2282
70. Gurlo A, Sahm M, Oprea A, Barsan N, Weimar U (2004) A p- to n-transition on α-Fe_2O_3-based thick film sensors studied by conductance and work function change measurements. Sens Actuators B-Chem 102(2):291–298
71. Dunstan PR, Maffeis TGG, Ackland MP, Owen GT, Wilks SP (2003) The correlation of electronic properties with nanoscale morphological variations measured by SPM on semiconductor devices. J Phys Condens Matter 15(42):S3095−S3112
72. Maffeis TGG, Owen GT, Malagu C, Martinelli G, Kennedy MK, Kruis FE, Wilks SP (2004) Direct evidence of the dependence of surface state density on the size of SnO_2 nanoparticles observed by scanning tunnelling spectroscopy. Surf Sci 550(1–3):21–25
73. Maffeis TGG, enny MP, Teng KS, Wilks SP, Ferkel HS, Owen GT (2004) Macroscopic and microscopic investigations of the effect of gas exposure on nanocrystalline SnO_2 at elevated temperature. Appl Surf Sci 234(1–4):82–85
74. Arbiol J, Gorostiza P, Cirera A, Cornet A, Morante JR (2001) In situ analysis of the conductance of SnO_2 crystalline nanoparticles in the presence of oxidizing or reducing atmosphere by scanning tunneling microscopy. Sens Actuators B-Chem 78(1–3):57–63
75. Barsan N, Schweizer-Berberich M, Gopel W (1999) Fundamental and practical aspects in the design of nanoscaled SnO_2 gas sensors: a status report. Fresenius J Anal Chem 365(4):287–304
76. Gurlo A, Riedel R (2007) In situ and operando spectroscopy for assessing mechanisms of gas sensing. Angewandte Chemie—Int Edn 46(21):3826–3848
77. Barsan N, Koziej D, Weimar U (2007) Metal oxide-based gas sensor research: how to? Sens Actuators B-Cheml 121(1):18–35
78. Windischmann H, Mark P (1979) A model for the operation of a thin-film tin oxide (SnOx) conductance-modulation carbon monoxide sensor. J Electrochem Soc 126(4):627–33
79. Schulz M, Bohn E, Heiland G (1979) Messung von Fremdgasen in der Luft mit Halbleitersensoren (Measurement of extraneous gases in air by means of semiconducting sensors). Tech Messen 46(11):405–14
80. Williams DE (1987) Conduction and gas response of semiconductor gas sensors. In: Moseley PT and Totfield BC (eds) Solid state gas sensors, Adam Hilger, Philadelphia, pp 71–123
81. Madou MJ, Morrison SR (1989) Chemical sensing with solid state devices. Academic Press, San Diego, p 556

82. Gas Sensors. Sberveglieri G (ed) 1992, Kluwer, Dordrecht, p 409
83. Jarzebski ZM, Marton JP (1976) Physical properties of tin(IV) oxide materials. II. Electrical properties. J Electrochem Soc 123(9):299–310
84. Sahm T, Gurlo A, Barsan N, Weimar U (2005) Basics of oxygen and SnO_2 interaction; work function change and conductivity measurements. In Eurosensors XIX, European conference on solid-state transducers, Barcelona
85. Tournier G, Pijolat C (1999) Influence of oxygen concentration in the carrier gas on the response of tin dioxide sensor under hydrogen and methane. Sens Actuators, B: Chem B61(1–3):43–50
86. Arnold MS, Avouris P, Pan ZW, Wang ZL (2003) Field-effect transistors based on single semiconducting oxide nanobelts. J Phys Chem B 107(3):659–663
87. Kalinin SV, Shin J, Jesse S, Geohegan D, Baddorf AP, Lilach Y, Moskovits M, Kolmakov A (2005) Electronic transport imaging in a multiwire SnO_2 chemical field-effect transistor device. J Appl Phys 98(4)
88. Szuber J, Czempik G, Larciprete R, Adamowicz B (2000) The comparative XPS and PYS studies of SnO_2 thin films prepared by L-CVD technique and exposed to oxygen and hydrogen. Sens Actuators, B: Chem B70(1–3):177–181
89. Figurovskaya EN, Kiselev VF, Vol'kenshtein FF (1965) Influence of chemisorption of oxygen on the work function and electrical conductivity of TiO_2. Doklady Akademii Nauk SSSR 161(5):1142–1145
90. Kiselev VF (1967) Borderline between physical and chemical adsorption. Zeitschrift fuer Chemie 7(10):369–378
91. Gopel W, Rocker G, Feierabend R (1983) Intrinsic defects of TiO_2(110)—interaction with chemisorbed O_2, H_2, CO, and CO_2. Phy Rev B 28(6):3427–3438
92. Heiland G (1954) Zum Einfluss von Wasserstoff auf die elektrische Leitfähigkeit von ZnO-Kristallen. Zeitschrift der Physik 138:459–464
93. Goepel W (1978) Reactions of oxygen with zinc oxide-(1010) surfaces. J Vac Sci Technol 15(4):1298–310
94. Fujitsu S, Koumoto K, Yanagida H, Watanabe Y, Kawazoe H (1999) Change in the oxidation state of the adsorbed oxygen equilibrated at 25 °C on ZnO surface during room temperature annealing after rapid quenching. Jpn J Appl Phys Part 1: Regular papers, Short notes and review papers 38(3A):1534–1538
95. Na BK, Walters AB, Vannice MA (1993) Studies of gas adsorptiongas adsorption on zinc oxide using ESR, FTIR spectroscopy, and MHE (microwave Hall effect) measurements. J Catal 140(2):585–600
96. Kiselev VF, Krylov OV (1987) Springer series in surface sciences, electronic phenomena in adsorption and catalysis on semiconductors and dielectrics. 7:279
97. McAleer JF, Moseley PT, Norris JOW, Williams DE (1987) Tin dioxide gas sensors. Part 1. Aspects of the surface chemistry revealed by electrical conductance variations. J Chem Soc, Faraday Trans 1: Phys Chem Condens Phases 83(4):1323–1346
98. Harrison PG, Willett MJ (1989) Tin oxide surfaces. 20. Electrical properties of tin(IV) oxide gel: nature of the surface conductance in air as a function of temperature. J Chem Soc, Faraday Trans 1: Phys Chem Condens Phases 85(8):1921–1932
99. Willett MJ (1991) Spectroscopy of surface reactions In: Moseley PT, Norris JO and Williams DE (eds) Techiques and mecahnism in gas sensing, Adam Hilger, Bristol, pp 61–107
100. Pulkkinen U, Rantala TT, Rantala TS, Lantto V (2001) Kinetic Monte Carlo simulation of oxygen exchange of SnO_2 surface. J Mol Catal A: Chem 166(1):15–21
101. Lantto V, Romppainen P (1987) Electrical studies on the reactions of carbon monoxide with different oxygen species on tin dioxide surfaces. Surf Sci 192(1):243–264
102. Roduner E (2006) Size matters: why nanomaterials are different. Chem Soc Rev 35(7): 583–592
103. Oprea A, Gurlo A, Barsan N, Weimar U (2009) Transport and gas sensing properties of In_2O_3 nanocrystalline thick films: a hall effect based approach. Sens Actuators B-Chem 139(2):322–328

104. Geistlinger H (1993) Electron theory of thin-film gas sensors Sens Actuators, B: Chem 17(1):47–60
105. Geistlinger H, Eisele I, Flietner B, Winter R (1996) Dipole- and charge transfer contributions to the work function change of semiconducting thin films: experiment and theory. Sens Actuators, B: Chem B34(1–3):499–505
106. Rothschild A, Komem Y (2003) Numerical computation of chemisorption isotherms for device modeling of semiconductor gas sensors. Sens Actuators B-Chem 93(1–3):362–369
107. Gurlo A, Barsan N, Ivanovskaya MùWeimar U, Gopel W (1998) In_2O_3 and MoO_3-In_2O_3 thin film semiconductor sensors: interaction with NO_2 and O_3. Sens Actuators B-Chem 47(1–3):92–99
108. Wahlstrom E, Vestergaard EK, Schaub R, Ronnau A, Vestergaard M, Laegsgaard E, Stensgaard I, Besenbacher F (2004) Electron transfer-induced dynamics of oxygen molecules on the TiO_2(110) surface. Science 303(5657):511–513
109. Gurlo A (2006) Interplay between O_2 and SnO_2: oxygen ionosorption and spectroscopic evidence of adsorbed oxygen. ChemPhysChem 7:2041–2052
110. Henderson MA, Epling WS, Perkins CL, Peden CHF, Diebold U (1999) Interaction of molecular oxygen with the vacuum-annealed TiO_2(110) surface: molecular and dissociative channels. J Phys Chem B 103(25):5328–5337
111. Bartolucci F, Franchy R, Barnard JC, Palmer RE (1998) Two chemisorbed species of O_2 on Ag(110). Phys Rev Lett 80(23):5224–5227
112. Iwamoto M, Yoda Y, Yamazoe N, Seiyama T (1978) Study of metal oxide catalysts by temperature programmed desorption. 4. Oxygen adsorption on various metal oxides. J Phys Chem 82(24):2564–2570
113. Tanaka K, Blyholder G (1972) Adsorbed oxygen species on zinc oxide in the dark and under illumination. J Phys Chem 76(22):3184–7
114. Zemel JN (1988) Theoretical description of gas-film interaction on tin oxide (SnOx). Thin Solid Films 163:189–202
115. Kolmakov A, Moskovits M (2004) Chemical sensing and catalysiscatalysis by one-dimensional metal-oxide nanostructures. Ann Rev Mater Res 34:151–180
116. Maier J, Gopel W (1998) Investigations of the bulk defect chemistry of polycrystalline tin(IV) oxide. J Solid State Chem 72(2):293–302
117. Gopel W, Schierbaum K, Wiemhofer HD, Maier J (1989) Defect chemistry of tin(IV)-oxide in bulk and boundary-layers. Solid State Ionics 32(3):440–443
118. Kamp B, Merkle R, Lauck R, Maier J (2005) Chemical diffusion of oxygen in tin dioxide: Effects of dopantsdopants and oxygen partial pressure. J Solid State Chem 178(10): 3027–3039
119. Kamp B, Merkle R, Maier J (2001) Chemical diffusion of oxygen in tin dioxide. Sens Actuators, B: Chem B77(1–2):534–542
120. Armelao L, Barreca D, Bontempi E, Canevali C, Depero LE, Mari CM, Ruffo R, Scotti R, Tondello E, Morazzoni F (2002) Can electron paramagnetic resonance measurements predict the electrical sensitivity of SnO_2-based film? Appl Magn Reson 22(1):89–100
121. Safonova O, Bezverkhy I, Fabrichnyi P, Rumyantseva M, Gaskov A (2002) Mechanism of sensing CO in nitrogen by nanocrystalline SnO_2 and SnO_2(Pd) studied by Mossbauer spectroscopy and conductance measurements. J Mater Chem 12(4):1174–1178
122. Morandi S, Ghiotti G, Chiorino A, Comini E (2005) FT-IR and UVUV-Vis-NIR characterisation of pure and mixed MoO_3 and WO_3 thin films. Thin Solid Films 490(1):74–80
123. Lenaerts S, Roggen J, Maes G (1995) FT-IR characterization of tin dioxide gas sensor materials under working conditions. Spectrochim Acta Part A Mol Biomol Spectrosc 51A(5):883–894
124. Pohle R, Fleischer M, Meixner H (2001) Infrared emission spectroscopic study of the adsorption of oxygen on gas sensors based on polycrystalline metal oxide films. Sens Actuators B-Chem 78(1–3):133–137
125. Sergent N, Gelin P, Perier-Camby L, Praliaud H, Thomas G (2003) Study of the interactions between carbon monoxide and high specific surface area tin dioxide: Thermogravimetric analysis and FTIR spectroscopy. J Therm Anal Calorim 72(3):1117–1126

126. Koziej D, Barsan N, Weimar U, Szuber J, Shimanoe K, Yamazoe N (2005) Water-oxygen interplay on tin dioxide surface: implication on gas sensing. Chem Phys Lett 410(4–6): 321–323
127. Di Nola P, Morazzoni F, Scotti R, Narducci D (1993) Paramagnetic point defects in tin dioxide and their reactivity with surrounding gases. Part 1—interaction of oxygen lattice centers with vapor-phase water, air, inert and combustible gases, as revealed by electron paramagnetic resonance spectroscopy. J Chem Soc, Faraday Trans 89(20):3711–3713
128. Lenaerts S, Honore M, Huyberechts G, Roggen J, Maes G (1994) In situ infrared and electrical characterization of tin dioxide gas sensors in nitrogen/oxygen mixtures at temperatures up to 720 K. Sens Actuators, B: Chem 19(1–3):478–482
129. Ghiotti G, Chiorino A, Boccuzzi F (1989) Infrared study of surface chemistry and electronic effects of different atmospheres on tin dioxide. Sens Actuators 19(2):151–7
130. Harbeck S (2005) Characterisation and functionality of SnO_2 gas sensors using vibrational spectroscopy. Ph.D. thesis, Faculty of Chemistry, Universität tübingen, http://w210.ub.uni-tuebingen.de/dbt/volltexte/2005/1693/, Tuebingen
131. Fonstad CG, Rediker RH (1971) Electrical properties of high-quality stannic oxide crystals. J Appl Phys 42(7):2911–2918
132. Samson S, Fonstad CG (1973) Defect structure and electronic donordonor levels in stannic oxide crystals. J Appl Phys 44(10):4618–4621
133. Lopez N, Prades JD, Hernandez-Ramirez F, Morante JR, Pan J, Mathur S (2010) Bidimensional versus tridimensional oxygen vacancy diffusion in SnO_{2-x} under different gas environments. Phys Chem Chem Phys 12(10):2401–2406
134. Hernandez-Ramirez F, Prades JD, Tarancon AùBarth S, Casals O, Jimenez-Diaz R, Pellicer EùRodriguez J, Morante JR, Juli MA, Mathur S, Romano-Rodriguez A (2008) Insight into the role of oxygen diffusion in the sensing mechanisms of SnO_2 nanowires. Adv Funct Mater 18(19):2990–2994
135. Boreskov GK (1964) The catalysis of isotopic exchange in molecular oxygen. Adv Catal 15:285–339
136. Safonova OV, Neisius T, Ryzhikov A, Chenevier B, Gaskov AM, Labeau M (2005) Characterization of the H_2 sensing mechanism of Pd-promoted SnO_2 by XAS in operando conditions. Chem Commun 41:5202–5204
137. Schmid W, Barsan N, Weimar U (2003) Sensing of hydrocarbons with tin oxide sensors: possible reaction path as revealed by consumption measurements. Sens Actuators B-Chem 89(3):232–236
138. Delabie L, Honore M, Lenaerts S, Huyberechts G, Roggen J, Maes G (1997) The effect of sintering and Pd-doping on the conversion of CO to CO_2 on SnO_2 gas sensor materials. Sens Actuators B-Chem 44(1–3):446–451
139. Dutta PK, De Lucia MF (2006) Correlation of catalytic activity and sensor response in TiO_2 high temperature gas sensors. Sens Actuators, B: Chem 115(1):1–3
140. Schmid W, Barsan N, Weimar U (2004) Sensing of hydrocarbons and CO in low oxygen conditions with tin dioxide sensors: possible conversion paths. Sens Actuators B-Chem 103(1–2):362–368
141. Hahn SH, Barsan N, Weimar U, Ejakov SG, Visser JH, Soltis RE (2003) CO sensing with SnO_2 thick film sensors: role of oxygen and water vapour. Thin Solid Films 436(1):17–24
142. Gurlo A, Sahm M, Oprea A, Barsan N, Weimar U (2004) A p- to n-transition on alpha-Fe_2O_3-based thick film sensors studied by conductance and work function change measurements. Sens Actuators B-Chem 102(2):291–298
143. Gurlo A, Barsan N, Oprea A, Sahm M, Sahm T, Weimar U (2004) An n- to p-type conductivity transition induced by oxygen adsorption on alpha-Fe_2O_3. Appl Phys Lett 85(12):2280–2282
144. Arulsamy AD, Elersic K, Modic M, Cvelbar U, Mozetic M (2010) Reversible carrier-type transitions in gas-sensing oxides and nanostructures. Chem Phys Chem 11(17):3704–3712
145. Gurlo A (2006) Interplay between O_2 and SnO_2: oxygen ionosorption and spectroscopic evidence for adsorbed oxygen. Chem Phys Chem 7(10):2041–2052

146. Hahn S (2002) SnO_2 thick film sensors at ultimate limits: performance at low O_2 and H_2O concentrations. Size reduction by CMOS technology, Ph.D. thesis, Faculty of Chemistry, Universität Tübingen, Tuebingen
147. Benitez JJ, Centeno MA, Merdrignac OMùGuyader J, Laurent YJ, Odriozola A (1995) DRIFTS chamber for in situ and simultaneous study of infrared and electrical response of sensors. Appl Spectrosc 49(8):1094–6
148. Benitez JJ, Centeno MA, dit Picard CL, Merdrignac O, Laurent Y, Odriozola JA (1996) In situ diffuse reflectance infrared spectroscopy (DRIFTS) study of the reversibility of CdGeON sensors towards oxygen. Sens Actuators, B: Chem B31(3):197–202
149. Safonova OV, Neisius T, Chenevier B, Matko I, Labeau M, Gaskov A (2004) In situ XAS studies on the effect of Pd and Pt clusters on the mechanism of SnO_2 based gas sensors. In 13th international congress on catalysis, Paris, France, July 2004
150. Gaidi M, Chenevier B, Labeau M, Hazemann JL In situ simultaneous XAS and electrical characterizations of Pt-doped tin oxide thin film deposited by pyrosol method for gas sensors application. Sens Actuators, B: Chem B120(1):313–315
151. Gaidi M, Labeau M, Chenevier B, Hazemann JL (1998) In situ EXAFS analysis of the local environment of Pt particles incorporated in thin films of SnO_2 semi-conductor oxide used as gas-sensors. Sens Actuators B-Chem 48(1–3):277–284
152. Gaidi M, Hazemann JL, Matko I, Chenevier B, Rumyantseva M, Gaskov A, Labeau M (2000) Role of Pt aggregates in Pt/SnO_2 thin films used as gas sensors—investigations of the catalytic effect. J Electrochem Soc 147(8):3131–3138
153. Sharma SS, Nomura K, Ujihira Y (1992) Moessbauer studies on tin-bismuth oxide carbon monoxide selective gas sensor. J Appl Phys 71(4):2000–5
154. Nomura K, Sharma SS, Ujihira Y (1993) Characterization of tin oxide films gas sensor by in situ conversion electron Moessbauer spectrometry (CEMS). Nucl Instrum Methods Phys Res, Sect B B76(1–4):357–9
155. Baraton M.-I, Merhari L (2005) Investigation of the gas detection mechanism in semiconductor chemical sensors by FTIR spectroscopy. Synth React Inorg, Met-Org, Nano-Met Chem 35(10):733–742
156. Baraton M-I, Merhari L (2004) Nanoparticles-based chemical gas sensors for outdoor air quality monitoring. Nano-Micro Interface 227–238
157. Baraton M-I (1996) FT-IR surface study of nanosized ceramic materials used as gas sensors. Sens Actuators, B: Chem B31(1–2):33–8
158. Baraton MI (1994) Infrared and Raman characterization of nanophase ceramic materials. High Temp Chem Processes 3:545–554
159. Baraton MI, Merhari L, Ferkel H, Castagnet JF (2002) Comparison of the gas sensing properties of tin, indium and tungsten oxides nanopowders: carbon monoxide and oxygen detection. Mater Sci Eng C-Biomimetic Supramolecular Syst 19(1–2):315–321
160. Baraton MI, Merhari L, Keller P, Zweiacker K, Meyer JU (1999) Novel electronic conductance CO_2 sensors based on nanocrystalline semiconductors. Materials research society symposium proceedings, (Microcrystalline and Nanocrystalline Semiconductors–1998) 536:341–346
161. Chiorino A, Ghiotti G, Prinetto F, Carotta MCùMalagu C, Martinelli G (2001) Preparation and characterization of SnO_2 and WOx-SnO_2 nanosized powders and thick films for gas sensing. Sens Actuators, B: Chem B78(1–3):89–97
162. Chiorino A, Ghiotti G, Prinetto F, Carotta MC, Gallana M, Martinelli G (1999) Characterization of materials for gas sensors. Surface chemistry of SnO_2 and MoOx-SnO_2 nano-sized powders and electrical responses of the related thick films. Sens Actuators B-Chem 59(2–3):203–209
163. Chiorino A, Ghiotti G, Carotta MC, Martinelli G (1998) Electrical and spectroscopic characterization of SnO_2 and Pd-SnO_2 thick films studied as CO gas sensors. Sens Actuators, B: Chem B47(1–3):205–212

164. Chiorino A, Ghiotti G, Prinetto F, Carotta MC, Martinelli G, Merli M (1997) Characterization of SnO_2-based gas sensors a spectroscopic and electrical study of thick films from commercial and laboratory-prepared samples. Sens Actuators, B Chem B 44(1–3):474–482
165. Popescu DA, Herrmann JM, Ensuque A, Bozon-Verduraz F (2001) Nanosized tin dioxide: spectroscopic (UV-VIS, NIR, EPR) and electrical conductivity studies Phys Chem Chem Phys 3(12):2522–2530
166. Canevali C, Mari CM, Mattoni M, Morazzoni F, Ruffo R, Scotti R, Russo U, Nodari L (2004) Mechanism of sensing NO in argon by nanocrystalline SnO_2: electron paramagnetic resonance, Mossbauer and electrical study. Sens Actuators, B: Chem B100(1–2):228–235
167. Canevali C, Mari CM, Mattoni M, Morazzoni F, Nodari L, Ruffo R, Russo U, Scotti R (2005) Interaction of NO with nanosized Ru-, Pd-, and Pt-doped SnO_2: electron paramagnetic resonance, Mossbauer, and electrical investigation. J Phys Chem B 109(15):7195–7202
168. Morazzoni F, Canevali C, Chiodini N, Mari C, Ruffo R, Scotti R, Armelao L, Tondello E, Depero LE, Bontempi E (2001) Nanostructured Pt-doped tin oxide films: sol-gel preparation, spectroscopic and electrical characterization. Chem Mater 13(11):4355–4361